

Growth of ZnO nanowires on retroreflector microspheres and the resulting light channeling and plasmonic properties.

S.M. Prokes¹, O.J. Glembocki¹, and Erin Cleveland*¹ and Hua Qi*¹,

*ASEE Postdoctoral Fellow, Washington, DC

¹Naval Research Laboratory, Washington, DC 20375.

We have investigated the growth of ZnO nanowires on curved BaTiO₃ retroreflector beads, as well as growth of ZnO nanowires on flat substrates. Results indicate that the growth of ZnO aligned nanowire arrays occurs farther away from the Zn source in the retroreflectors, while the results are opposite for the flat Si substrates. In the case of the ZnO nanowires on flat Si, the nanowires formed in nearly aligned arrays are short and significantly thicker, suggesting that the growth occurs both longitudinally and laterally in this process, which is not the case for the growth on the retroreflector beads. The SERS response of the nanowire arrays on the retroreflectors has been compared to random nanowires on flat Si substrates, and results show that the signal strength is 29 times greater in the case of the wires grown on the retroreflectors. Since one would only expect a factor of 4 enhancement due to the light reflecting properties of the retroreflector, it is believed that the enhancement in the SERS signal is due to light channeling by the aligned nanowire arrays.

1. Introduction

Optically based sensing provides advantages over electronic sensing because the sensor can be made covert and passive. The concept of using Raman scattering (RS) and surface enhanced Raman scattering for chemical detection is shown in Figure 1. In RS, laser light is scattered from a chemical of interest and the vibrational modes of the chemical red and blue shift the frequency of the scattered light, producing a spectrum of lines that are characteristic of the chemical probe. Because molecules and solids have unique combinations of atoms, the RS results in a spectrum that is a unique fingerprint for any molecule or solid. In Fig 1b, the spectra are for liquids of acetone and DMMP. These liquids are usually difficult to discriminate using electronic sensors, which are sensitive to classes of molecules.

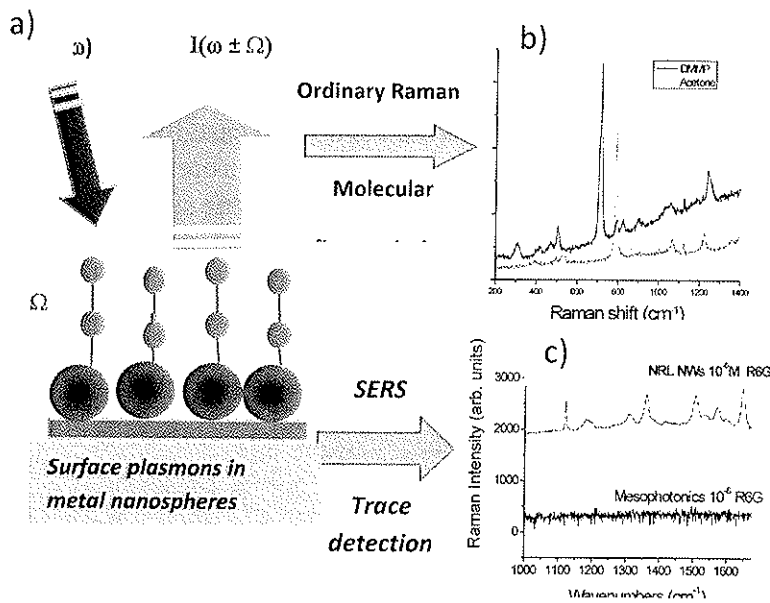


Figure 1. Raman scattering for liquids of acetone and DMMP (top right) and Surface enhanced Raman scattering for Rh6G (bottom right) using NRL dielectric NWs and commercial Mesophotonics substrates. . The cartoon on the left shows the SERS effect.

intersecting nanoparticles. We have previously developed SERS materials based on dielectric core/metal sheath nanowires (NWs), which have shown to be very effective in the detection of trace levels of chemicals, due to plasmon coupling in crossed regions of the NWs [2,3], as well as due to the interaction of the NW with the substrate [4]. An example of the SERS sensitivity of these NWs compared to commercial SERS substrates is shown in Fig. 1c. Shown is a comparison of the SERS spectrum of trace amounts of Rh6G, (which is a standard SERS dye) for a commercial Mesophotonics substrate and the dielectric core NWs. The signal is quite evident in the case of the NWs but not apparent for the commercial substrate.

The graph shows that it is easy to discriminate between the two. A major issue for ordinary Raman scattering is that its cross-sections are very small resulting in low sensitivity ($1E^{-8}$ of the exciting laser), which is a problem for the detection of trace amounts chemicals. Shown in Fig 1a is the approach that is used to enhance the Raman signal. Nanotextured metals such as Ag and Au have the property that when exposed to light, surface plasmons are generated which interact with the laser light to increase the local electric fields and thus the scattering intensity at the surface [1]. This leads to Raman enhancements as high as 10^6 from the individual nanoparticles and as high as 10^{12} from regions of

Use of retroreflectors to alter the spatial profiles of Surface Enhanced Raman scattering

A key application of SERS would involve standoff detection of chem./bio hazards. To achieve this, standoff distances should be greater than 10m. One of the critical issues that inhibits the easy applications of SERS to standoff applications is the fact that the SERS process is an inelastic scattering process which radiates light outward into a sphere. Thus any remote sensing approach will detect only a small solid angle defined by the diameter of the detector and the distance of that source. Significant improvements in signal strength and ultimately in sensitivity and detection times may be achieved if the scattered radiation is directed back toward the detection system.

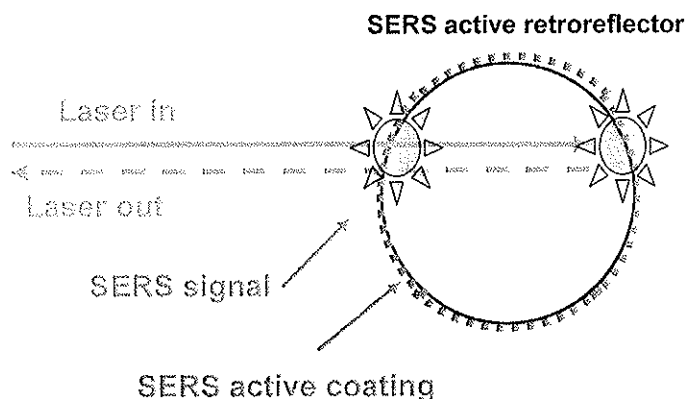


Figure 2. Schematic representation of a SERS active retroreflector bead and the increased light collection.

producing Raman scattering at the front of the retroreflector as well as at the back. We would expect to detect not only the back scattered SERS signal, but also the forward scattered signal. In addition, the retroreflector will redirect the exciting laser beam back toward the source. This adds an extra pass that will produce additional SERS. Thus, in this paper, we have investigated the formation of SERS media by incorporating the retroreflector beads with our already developed dielectric core/metal sheath nanowires in order to potentially enhance the return SERS signal from this structure.

2. Experimental details

The ZnO nanowires were grown in a tube furnace, under atmospheric conditions, using solid Zn pellets. Argon gas flow was used to carry the Zn vapor to the substrates, which were placed at various distances from the Zn solid source. We also used BaTiO₃ retroreflector beads, which have an index of refraction of 1.9, as the substrates for the ZnO nanowire growth. The beads varied in sizes from 70 to 500 μ m, as determined by SEM. The retroreflector beads were attached to a Si substrate using a high temperature alumina paste and the substrates were then loaded into the

A powerful optical technique for returning light back to the source is retroreflection, in which the optical element is designed to reflect light back along its incident path. The simplest possible retroreflector is a high index bead that is routinely utilized in highway and runway construction to redirect light back toward the source. This approach clearly offers an alternative media for the fabrication of SERS substrates. It would have the advantage of having a well determined size, providing a very efficient use of the incident and scattered light collection and finally be easily located in standoff applications. Figure 2 shows this concept for an incident laser

furnace. We also investigated the growth of the ZnO nanowires on flat Si substrates in order to compare the growth conditions. In both cases, the growth of the ZnO nanowires was by the vapor solid (VS) growth since no metal catalyst was deposited on the substrate prior to growth. The growth was performed at 560°C for 30 minutes. In order to investigate the SERS properties of these structures, we then deposited 15nm of Ag by atomic layer deposition (ALD) and SERS testing was performed using a standard benzenethiol (BZT) molecule. In addition, we performed COMSOL electric field calculations in order to compare to the experimental results.

The SERS were performed using a Delta Nu system which consists of an Olympus Microscope and a Raman spectrometer equipped with a thermoelectrically cooled CCD. The 785 nm line of Ti : Sapphire laser was used as the excitation source to detect the SERS strength dependence on a single NW/silver composite. The microscope utilized a 50X 0.75 NA objective for focusing the laser light. The spectra were collected with a laser power of 3 mW at the sample.

3. Growth Results:

An optical and SEM images of the retroreflector beads is shown in Figure 2. Note that the beads vary in size from 70 to 500 μm .

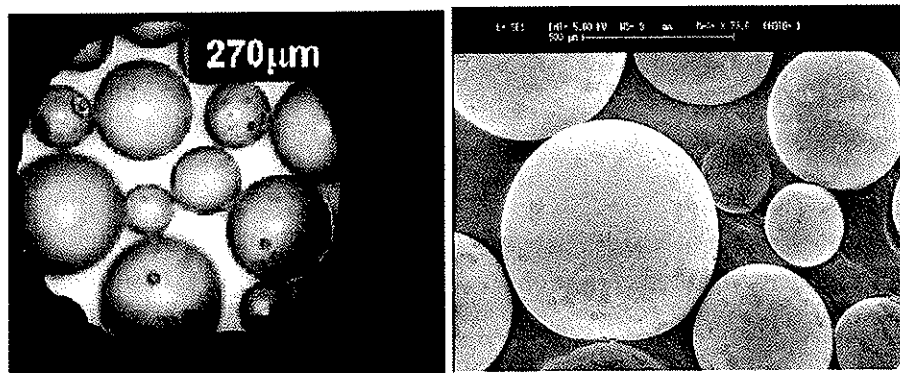


Figure 2. Optical and SEM images of retroreflector beads attached to alumina on Si.

In order to investigate the growth of ZnO nanowires (NWs) on these curved structures, we first investigated the ZnO NW growth on flat Si substrates in order to compare the growth parameters. Shown in Figure 3 are growths of ZnO structures as a function of distance from the solid Zn source, all growth performed at 560°C for 30 minutes. As can be seen, the farthest growth from the solid source leads to NWs which are greater than 10 microns in length, with a diameter in the 100nm range. As the distance between the substrate and the source decreases, the NWs get more defective and shorter, but when one examines the closest substrate to the solid Zn source, one finds a number of regions which contain more aligned NWs, that are in the 200 nm diameter range, but which are significantly shorter, usually between 1-2 microns. Since the temperature difference between the most outlying substrate and the nearest substrate is differs by less than 5°C, it is clear that the large difference in the NW morphologies is due to the amount of Zn to O vapor which reaches a specific

substrate. In the case of the closest substrates, the growth of the NWs most likely occurs at the tip as well as at the sidewalls, leading to shorter and wider nanowires, while those that grow farthest away exhibit much faster growth along the nanowire length and minimal growth laterally.

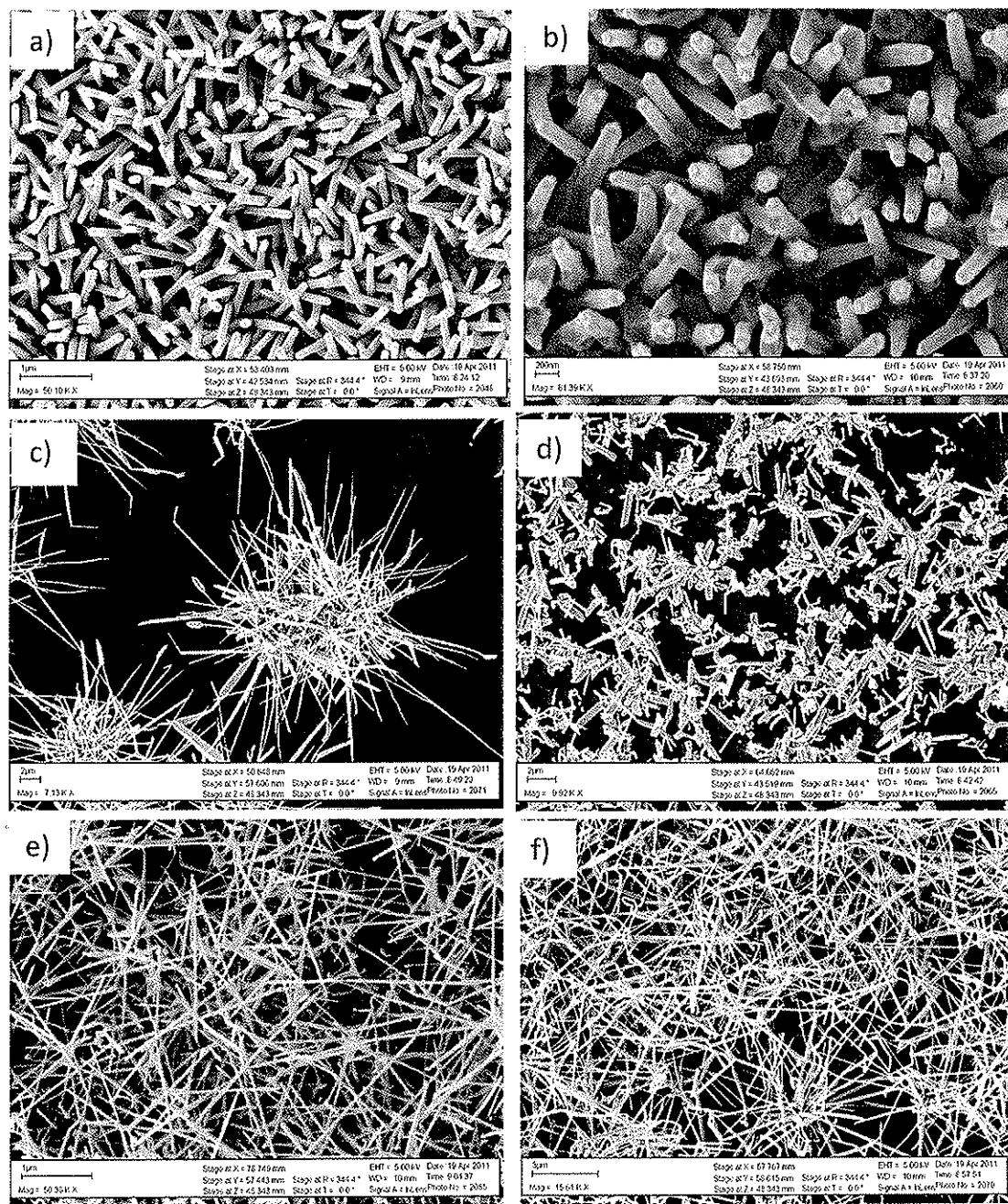


Figure 3: ZnO NW growth as a function of distance from the Zn source on a flat Si substrate. a) and b) are the closest and f) is the farthest away from the Zn source.

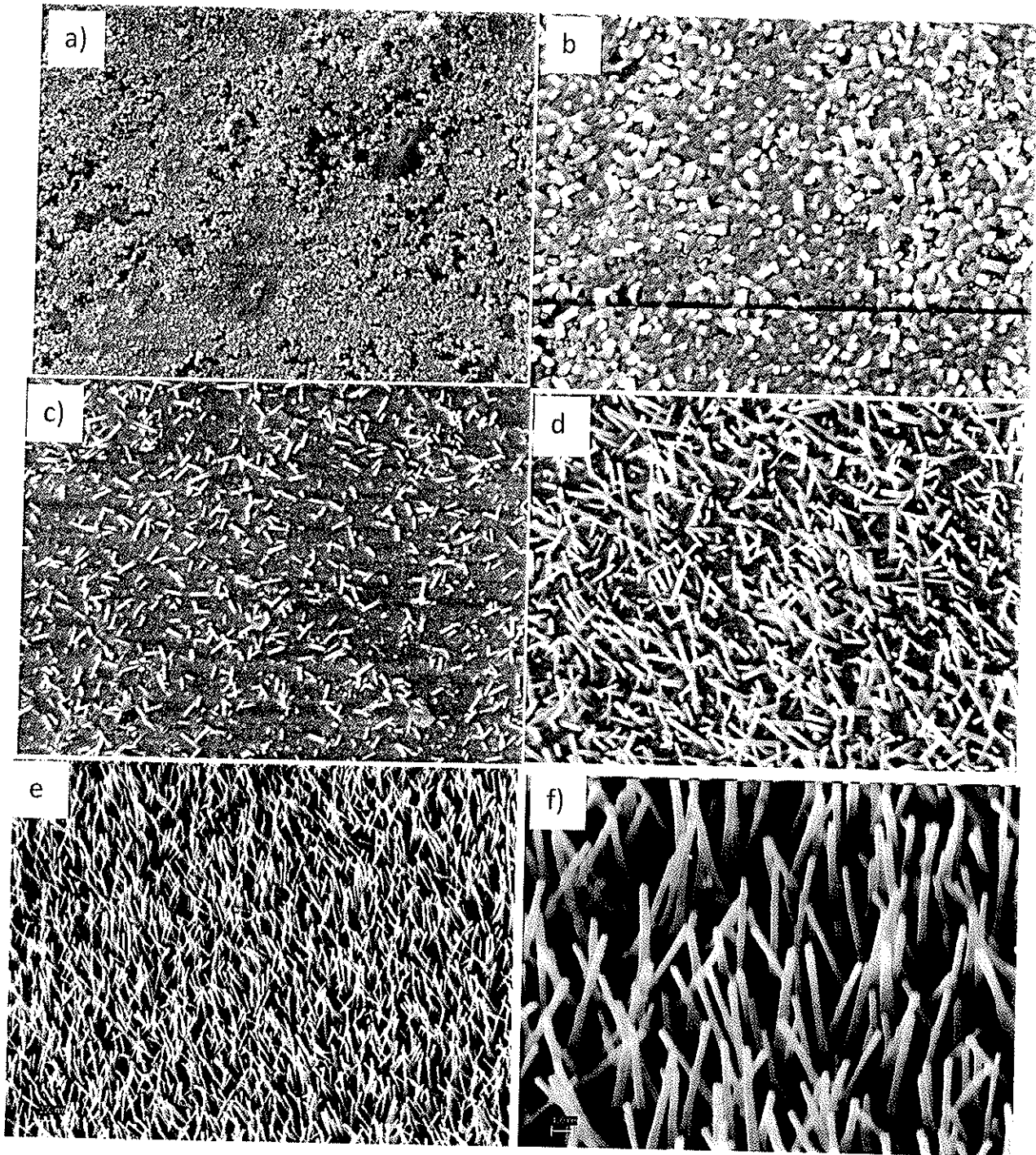


Figure 4: ZnO NW growth on retroreflectors as a function of distance from the Zn source. a) is the closest e) and f) are the farthest away from the Zn source.

One can now examine the growth behavior of the ZnO NW on the curved retroreflector beads, where once again, a number of substrates at various distances from the solid source were examined. Results for the ZnO/retroreflector growth are shown in Figure 4. As can be seen, the substrate closest

to the Zn source exhibits no NW growth and only a thick layer of ZnO film can be seen. As one moves away from the Zn source, however, the beginning of NW growth is evident, shown in Fig. 4b. As the distance increases, the NWs density increases and for the substrate farthest from the source, one can see the growth of shorter, aligned NWs. In this case, it is clear that it appears that it is more difficult nucleate the ZnO NWs on these retroreflectors and thus the initial growth results in a high rate of deposition of a ZnO film consisting of ZnO crystallites. As the amount of Zn vapor decreases farther away from the source, however, the nucleation of the NW begins and farthest away from the source, where the vapor supply is the lowest, aligned ZnO nanowires can be formed. Note that in this case, the nanowires are in the 100nm range and they are less than 3 microns in length. The retroreflector can be fully covered with these nanowire arrays, as shown in Figure 5.

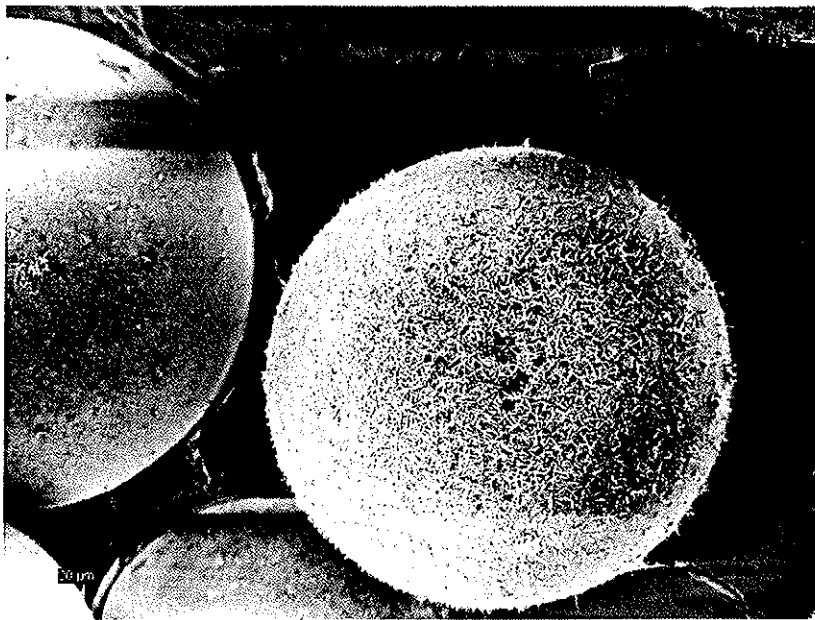


Figure 5: ZnO NW growth on retroreflectors. Note that the retroreflector can be fully covered with ZnO NWs.

4. Plasmonic Properties

Once these structures were formed, a thin layer of Ag was deposited onto them in order to evaluate their plasmonic properties. The Ag was deposited via ALD, which produces conformal and very uniform thin films, as shown in Figure 6 in the case of Ag deposition on the retro shown in Fig. 4f. As can be seen, the metal coverage on each NW is complete and uniform, which is important in order to examine the SERS behavior of these structures. Once formed, these Ag/ZnO NW composites were introduced into aBZT and allowed to form a single self assembled monolayer. The SERS response for the retroreflector sample shown in Fig. 6 which has the aligned

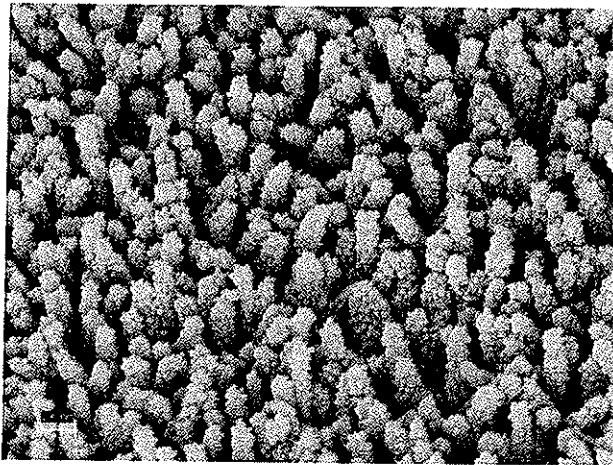


Figure 6: Ag thin film on ZnO NW growth on retroreflectors, performed by ALD. Note that the NWs are fully covered with the Ag.

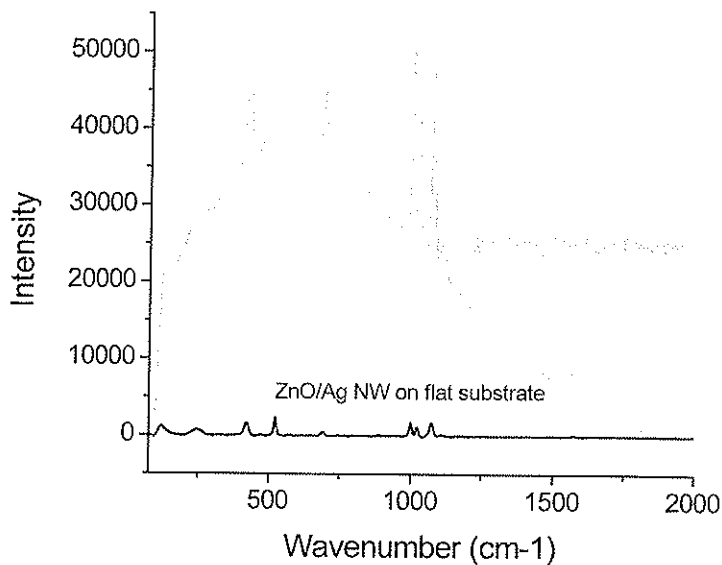


Figure 7. The SERS spectra for a self assembled monolayer of BZT applied to a plasmonic retroreflector (top) and to a flat Si substrate coated with Ag/ZnO nanowires.

NW arrays was compared to the SERS response of random ZnO NWs grown on Si, similar to those samples shown in Figure 1f.

The results are shown in Figure 7. As can be seen, a much stronger response is evident from the nearly aligned NWs on the retroreflectors compared to the random horizontal NW composites. Note that there is a factor of 29 increase in the SERS signal from the nanowires grown directly on the retroreflectors, compared to the same nanowires grown on Si. This gain cannot be explained by simple optical considerations as discussed below.

An estimation of the effect of using a retroreflector as a substrate for SERS can be made by doing an optical simulation of a point source by itself compared to a point source on the surface of a corner cube, which will behave in a manner similar to a retroreflector. Shown in Figure 8 are the results of such a simulation. Figure 8a shows the light pattern for a point source and the measured intensity at a plane located at an arbitrary distance from the point source, shown as a blue line. At this position, only 19.62% of the source power is detected. It is important to note that this light is the back scattered light. The forward scattered light is lost. If on the other hand, the point source is placed on the surface of a corner cube, the forward scattered light is redirected through the corner cube into a narrower cone and at the same

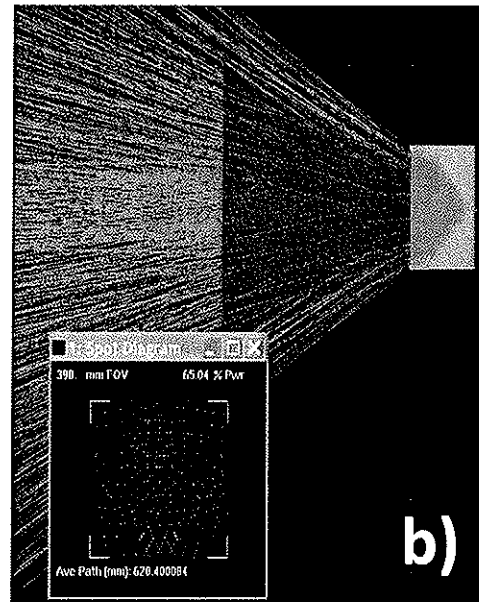
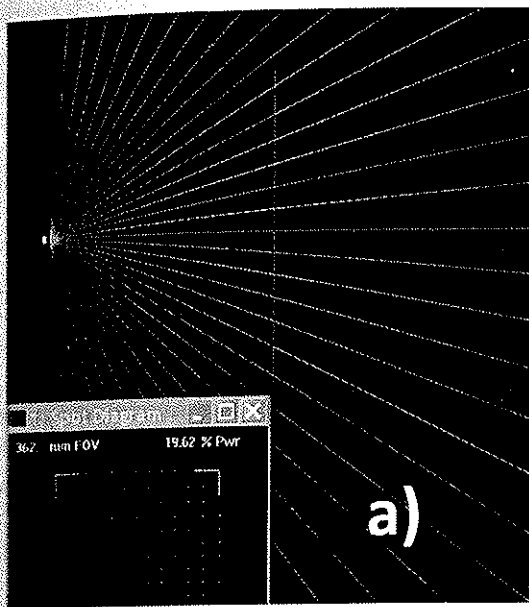


Figure 8. Simulated light scattering a) from a point source and b) from a point source on the surface of a corner cube. In both cases, the inset shows the intensity distribution on a plane (blue line) located away from the point source.

location, we detect 65.04% of the source intensity from the recovery of the forward scattered light. This gain is in addition to the backscattered intensity which is 19.62% of light intensity. Hence, the theoretical gain from using a retroreflector as a substrate is $GR = (\text{Back scattered} + \text{forward scattered}) / (\text{back scattered}) = 4.31$. Thus, one would expect the SERS enhancement to increase only by a factor of 4, which is clearly not the case.

To investigate this effect, we have done 3D calculations of the SERS enhancement for parallel wires, which is shown in Figure 9. As can be seen, the top view shows an ordered, closely

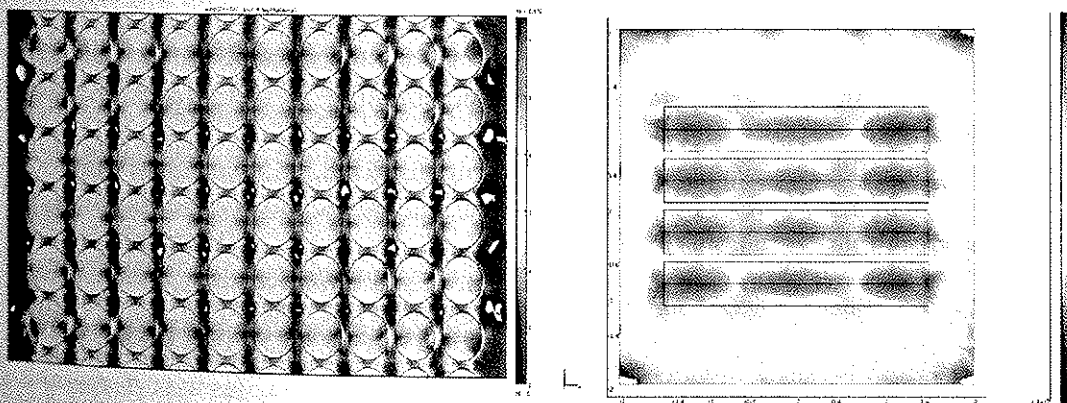


Figure 9. Figure 5 COMSOL simulations of the plasmonic coupling of parallel Si NWs; (a) top view; (b) side view.

spaced NW array with plasmon coupling “hot” spots between the wires. The side view shows that the plasmon coupling is along the whole length of the wire, resulting in a type of light channeling effect, as we have seen in the NW arrays on the retroreflectors.

The current hypothesis for the very high gain is that the nanowires are very closely spaced and nearly parallel to each other (see Fig. 4f). Under these conditions, the plasmonic effects would confine the electric fields to regions between the wires. This would result in much more directionality to the light scattering and the SERS light would enter the retroreflector as nearly parallel light. This would lead to much more light being recovered at our detector.

5. Conclusion

The growth of ZnO nanowires on curved BaTiO₃ retroreflector beads has been performed for the first time. Results indicate that the growth of ZnO aligned nanowire arrays occurs much farther away from the Zn source on the curved retroreflectors, compared to the growth on flat Si substrates. In the case of the ZnO nanowires on flat Si, the nanowire arrays formed were short and significantly thicker, suggesting that the growth proceeds both longitudinally and laterally, which is not the case for the growth on the retroreflector beads. The SERS response of the nanowire arrays on the retroreflectors has been compared to random nanowires on flat Si substrates, with results showing that the signal strength is 29 times greater in the case of the wires grown on the retroreflectors. Since one would only expect a factor of 4 enhancements due to the light reflecting properties of the retroreflector, it is believed that the enhancement in the SERS signal is due to light channeling by the aligned nanowire arrays.

6. Acknowledgments

The authors would like to acknowledge Alice King, Madhu Gowda, Josh Caldwell and Ron Rendell for helpful discussions.

7. References

- [1] Kottmann, J. P. Martin O. J. F. “Plasmon resonant coupling in metallic nanowires” *Optics Express* 8, 655-663 (2001).
- [2] Prokes, S.M., Glembocki, O.J., Rendell, R.W., and Ancona, M.G., “Enhanced plasmon coupling in crossed dielectric/metal nanowire composite geometries and applications to surface-enhanced Raman spectroscopy”, *Appl. Phys. Lett.* 2007,**90**, 093105.
- [3] S.M. Prokes, H.D. Park*, O.J. Glembocki, D. Alexson** and R.W. Rendell, “Plasmonic behavior of Ag/dielectric nanowires and the effect of geometry *Appl. Phys. Lett.* **94**, 093105 (2009)
- [4] O.J. Glembocki, R.W. Rendell, S.M. Prokes, D.A. Alexson, A. Fu* and M.A. Mastro, “Dielectric-Substrate interactions with metal/dielectric nanowires composites in surface-enhanced Raman spectroscopy”, *Phys. Rev. B* **80**, 1, (2009).